

LA-5917-MS

Informal Report

CIC-14 REPORT COLLECTION
**REPRODUCTION
COPY**

UC-20
Reporting Date: March 1975
Issued: June 1975

12 3

Ion Tail Filling in Laser-Fusion Targets

by

Dale B. Henderson



Los Alamos
scientific laboratory
of the University of California
LOS ALAMOS, NEW MEXICO 87544

An Affirmative Action/Equal Opportunity Employer

In the interest of prompt distribution, this report was not edited by the Technical Information staff.

Printed in the United States of America. Available from
National Technical Information Service
U S Department of Commerce
5285 Port Royal Road
Springfield, VA 22151
Price: Printed Copy \$4.00 Microfiche \$2.25

This report was prepared as an account of work sponsored by the United States Government. Neither the United States nor the United States Energy Research and Development Administration, nor any of their employees, nor any of their contractors, subcontractors, or their employees, makes any warranty, express or implied, or assumes any legal liability or responsibility for the accuracy, completeness, or usefulness of any information, apparatus, product, or process disclosed, or represents that its use would not infringe privately owned rights.

ION TAIL FILLING IN LASER-FUSION TARGETS

by

Dale B. Henderson

ABSTRACT

Thermonuclear burn begins in laser-fusion targets with the collapse of the imploding fuel shell. At this instant the ion velocity distribution is non-Maxwellian, requiring correction to the commonly used computer simulation codes. This correction is computed and compared with that arising from the loss of fast ions in marginal ($\rho R < 0.01 \text{ gm cm}^{-2}$) targets.



Thermonuclear burn of laser-fusion targets is generally thought of as commencing when a shell of DT (deuterium-tritium) fuel collapses at the central point. This shell may either be present initially or it may be formed through accumulation and compression of an initially homogeneous fuel.¹ At the instant of collapse, the velocity distribution of fuel ions may be thought of as a delta-function in speed: ions moving in all directions but with a common speed equal to that at which the shell moved inward.

In computer calculations of the implosion and burn,^{2,3} however, the velocity distribution is not taken into proper account. Instead, the ion fluid is taken to always have a Maxwellian distribution with the corresponding fusion reactivity $\langle \sigma v \rangle_M$. Because the fusion target may disassemble on a time scale comparable to that on which the ion distribution relaxes, it is important to study the relaxation and the corresponding values of fusion reactivity $\langle \sigma v \rangle$. In this report we describe a multispecies Fokker-Planck computer code developed for this purpose. We present calculations of the magnitude of the result which may be used to postcorrect the usual computer simulations. We also compare this effect with another related correction: the loss of ions from the tail of the distribution.⁴

METHOD

We use a Fokker-Planck code based on the work

of Rosenbluth, MacDonald, and Judd.⁵ We recast their Eqs. 20 and 21 in an obvious way by moving the summation signs to obtain

$$\frac{1}{\Gamma_a} \left[\frac{\partial g_a}{\partial t} \right]_c = - \frac{\partial}{\partial v^i} \left[g_a \sum_b \frac{m_a + m_b}{m_b} \frac{\partial \langle v^{-1} \rangle_b}{\partial v^i} \right] + \frac{1}{2} \frac{\partial^2}{\partial v^i \partial v^j} \left[g_a \sum_b \frac{\partial^2 \langle v \rangle_b}{\partial v^i \partial v^j} \right],$$

with

$$\Gamma_a = 4\pi e^4 Z_n \Lambda / m_o^2,$$

$$\langle v^{-1} \rangle_b(\vec{v}) = \int d\vec{v}' g_b(v') |\vec{v} - \vec{v}'|^{-1},$$

$$\langle v \rangle_b(\vec{v}) = \int d\vec{v}' g_b(v') |\vec{v} - \vec{v}'|,$$

where g is the distribution function and all the symbols are as customarily used and as defined in Ref. 4.

We specialize to the isotropic case by explicitly performing the angular integrations. We then nondimensionalize the equations and perform the indicated differentiations. The variables transform to

$$\begin{aligned} v &= v \xi \\ g &= v^{-3} G \\ t &= [v^3 / 2\pi \Gamma_1] \tau \end{aligned}$$

where ξ , G , and τ are dimensionless and Γ_I is the initial value of Γ_a . (In single-species problems, Γ is a constant). In these variables the equations become

$$\begin{aligned} \frac{\partial G_a}{\partial \tau} &= [\Gamma_a / \Gamma_I] \sum_b \left\{ G_a \left[2 \left(\frac{m_a}{m_b} \right) G_b \right] \right. \\ &+ \frac{\partial G_a}{\partial \xi} \left[2 \left(\frac{m_a}{m_b} \right) \xi^{-2} J_{2,b}(\xi) - \frac{2}{3} \xi^{-4} J_{4,b}(\xi) \right. \\ &\quad \left. \left. + \frac{4}{3} \xi^{-1} (J_{1,b}(\infty) - J_{1,b}(\xi)) \right] \right\} \\ &+ \frac{\partial^2 G_a}{\partial \xi^2} \left[\frac{2}{3} \xi^{-3} J_{4,b}(\xi) + \frac{2}{3} (J_{1,b}(\infty) - J_{1,b}(\xi)) \right], \end{aligned}$$

$$\text{where } J_{n,b}(\xi) \equiv \int z^n g_b(z) dz.$$

The equations have been encoded in this form.⁶ Two useful auxiliaries are the density

$$n_a = 4\pi J_{2,a}(\infty), \text{ and mean energy}$$

$$\epsilon_a \equiv \frac{3}{2} k T_a = \left[\frac{1}{2} m_a v^2 \right] J_{4,a}(\infty) / J_{2,a}(\infty).$$

A better nondimensionalization, at least for reporting results, is one using the density-time product (nt) as the independent variable. This scaling makes the evolution self-similar for problems not involving the loss of particles. An equivalent scaling uses Spitzer's value for the mean collision time,⁷ t_c :

$$v^{-1} \equiv t_c = m^{1/2} (3kT)^{3/2} / 8 \times 0.714 \pi n e^4 \ln \Lambda.$$

The number of mean collision times (vt), which is useful for interpretations, and the product (nt), which is useful for applications are simply related as

$$vt = nt \times [0.714(4\pi e^4 / m^2) \ln \Lambda (3/2 kT/m)^{3/2} / \sqrt{2}],$$

where the square bracket is a constant for many problems.

The fusion reactivity $\langle \sigma v \rangle$ is computed by simple quadrature over the distribution function $g(v)$. The values of σ used are obtained from the five parameter fit of Duane.⁸ Since the evolving function $g(v)$ is a function of (nt) or (vt), so is its quadrature $\langle \sigma v \rangle$.

The fractional burnup

$$f = \int \frac{1}{2} n \langle \sigma v \rangle dt$$

is also clearly a function of (nt) or (vt) for problems with a constant density n . Note that we are assuming $f \ll 1$ and ignore fuel depletion. One of our results will be that the ion-tail filling effect is unimportant in cases giving appreciable fractional burnup.

In our computations we have evaluated $\ln \Lambda$ with the mean energy ϵ . This is equivalent to assuming equal electron and ion temperatures, which is probably not correct in most implosion problems. Separate values of electron temperature would involve only different values of $\ln \Lambda$, amounting to a scaling in time. For the sake of simplicity we have not included these small effects. The results following were all computed for a single average DT ion, without electrons. The computer code is, however, more general allowing many species as described.

The relaxation of $\langle \sigma v \rangle$ toward its asymptotic value $\langle \sigma v \rangle_M$, corresponding to a Maxwellian ion distribution, is shown in Fig. 1 for a number of cases. In each case the temperature T is that of the Maxwellian; the initial beam speed is $v = (3kT/m)^{1/2}$.^{1,2} The horizontal lines are the asymptotic values $\langle \sigma v \rangle_M$. From the figure we see that the relaxation requires more collision times at the lower energies, because of the steepness of the cross-section σ at lower energies. The $T = 20$ -keV case is interesting in that it shows a small (5%) overshoot with the relaxation to the asymptotic value coming from above. The time conversion factors and the initial and asymptotic values of $\langle \sigma v \rangle$ are listed in Table I.

In Fig. 2 we plot the distribution function $g(v)$ as it relaxes toward the Maxwellian. The plot is for the $T = 6$ -keV case, but is really self-similar if scaled for different energies. We see that even after nearly 100 mean collision times, the deviation

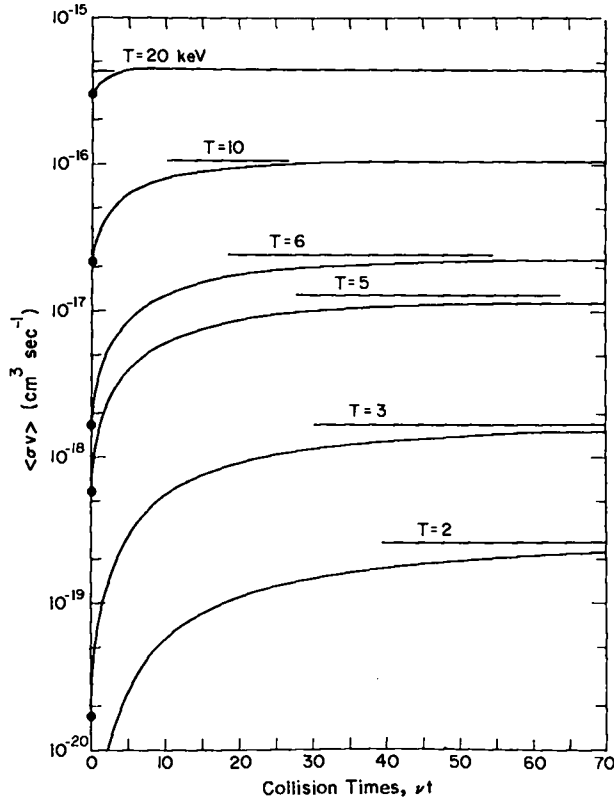


Fig. 1 Time evolution of the fusion reactivity $\langle \sigma v \rangle$ for various temperatures T.

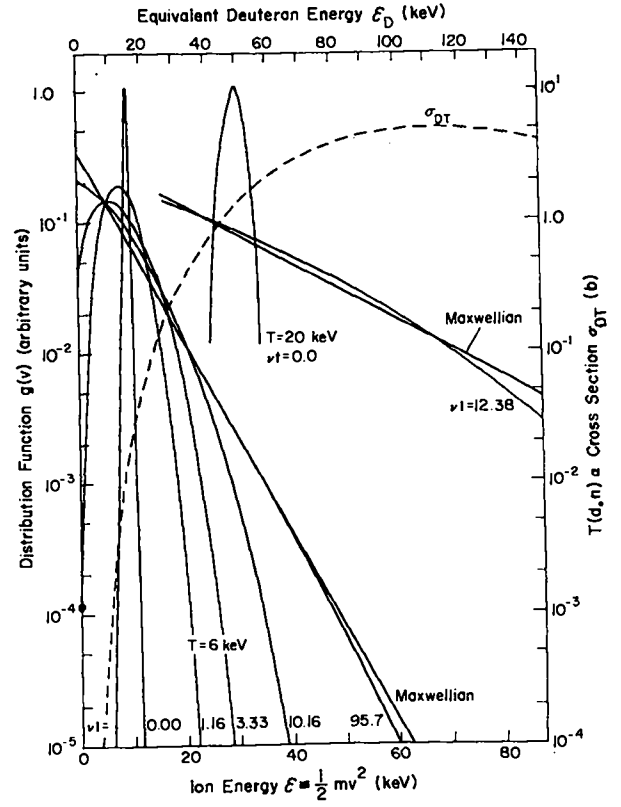


Fig. 2 Evolution of the distribution function $g(v)$ vs ion energy $\epsilon = \frac{1}{2} M v^2$. Overlaid is the fusion reaction cross section for DT.

TABLE I

T	$(nt)/(vt)$	$\langle \sigma v \rangle_0$	$\langle \sigma v \rangle_M$	$\langle \sigma v \rangle_0 / \langle \sigma v \rangle_M$
keV	cm ⁻³ sec	cm ³ sec ⁻¹	cm ³ sec ⁻¹	—
2	1.7×10^{10}	4.8×10^{-22}	2.6×10^{-19}	0.0018
3	3.0×10^{10}	1.7×10^{-20}	1.7×10^{-18}	0.0097
5	6.6×10^{10}	5.6×10^{-19}	1.3×10^{-17}	0.045
6	8.7×10^{10}	1.70×10^{-18}	2.4×10^{-17}	0.070
10	1.9×10^{11}	2.1×10^{-17}	1.9×10^{-16}	0.20
20	5.4×10^{11}	2.9×10^{-16}	4.2×10^{-16}	0.69

Time Conversion Factors, Initial Reactivity $\langle \sigma v \rangle_0$, Asymptotic or Maxwellian Reactivity, and their Ratio for Various Temperatures

from Maxwellian is appreciable at 10 times the thermal energy. Overlaid on the plot is a plot of the DT cross section σ , scaled in the energy coordinate as is appropriate.

Also plotted in Fig. 2 is the distribution for the $T = 20$ -keV case initially, asymptotically, and at $\nu t = 12.38$ which corresponds to the maximum value of $\langle \sigma v \rangle$. From the figure it is clear that the relative overpopulation of $g(v)$ adjacent to the initial delta-function is more important than the relative underpopulation in the far tail which lies largely beyond the maximum in σ . This explains the interesting overshoot.

The initial delta-functions used here were actually narrow Gaussians in speed with a width equal to $1/25$ of the mean speed. Values of $1/10$, $1/20$, and $1/40$ were also tried in order to verify that no effects were evident in the results of interest. That is, the beam spreads from a " $1/25$ " shape to approximately a " $1/10$ " shape in a small fraction of a collision time, $\nu t \ll 1$.

BURNUP

In Fig. 3 we show the evolution of $\langle \sigma v \rangle$ and its integral, the fractional burnup f , on linear scales, plotted against linear scales of time (νt)

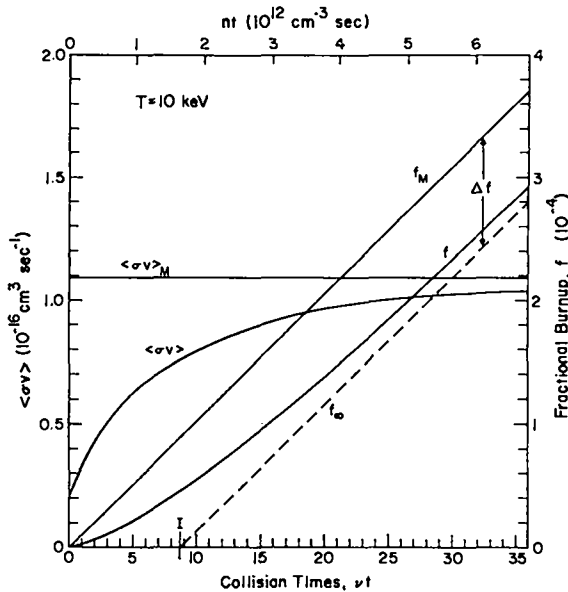


Fig. 3 Linear plot of the evolution of $\langle \sigma v \rangle$ and the fractional burnup f for the $T = 10$ -keV case.

and also (nt) . The plot is for the 10 -keV case, but illustrates a convenient parameterization of the results. Comparing the fractional burnup f with the a priori burnup f_M which would have occurred had the Maxwellian $\langle \sigma v \rangle_M$ applied for all time, we note that f becomes parallel to f_M as $\langle \sigma v \rangle$ saturates. For problems with relatively long burn-times, it is convenient to simply subtract off the "lost burnup" Δf from the burnup computed by the simulation code. This corrects for the code's assuming Maxwellian ion distributions at all times.

Alternatively, we could think of suppressing the start of burn (at the Maxwellian rate) by a relaxation time or induction time

$$(nt)_I = \Delta f / \frac{1}{2} \langle \sigma v \rangle_M,$$

which is indicated by the intercept "I" in the figure. Clearly, cases which proceed to large fractional burnup

$$f \gg \Delta f$$

or to large burn-time t_B ,

$$(nt)_B \gg (nt)_I$$

will not need significant corrections.

Computed values of Δf and $(nt)_I$ are listed in Table II for various temperatures T . The negative entries for $T = 20$ keV correspond to the overshoot in $\langle \sigma v \rangle$. The comparison of the a priori f from a hydrodynamics/burn calculation with Δf as computed here would seem to be the better test of whether a correction is needed, because of the possibility of bootstrap heating raising $\langle \sigma v \rangle$ with time as the burn ensues. On the other hand, Table II reveals a remarkable constancy in the values of $(nt)_I$ for the various temperatures of interest. As a handy rule of thumb, we conclude that corrections are not required for cases giving $(nt)_B$ for the burn much in excess of $10^{12} \text{ cm}^{-3} \text{ sec}$.

A more complete description of the results would be plots of the burnup vs time. A convenient representation of the time is the a priori fractional burnup for a Maxwellian distribution

$$f_M = \frac{1}{2} \langle \sigma v \rangle_M (nt).$$

TABLE II

T (keV)	Δf	$(nt)_I$ ($10^{11} \text{ cm}^{-3} \text{ sec}$)	$(vt)_I$
2	7.8×10^{-8}	5.9	36.
3	7.2×10^{-7}	8.4	28.
5	8.5×10^{-6}	13.1	20.
6	1.8×10^{-5}	14.8	17.
10	8.9×10^{-5}	16.3	8.7
20	-1.5×10^{-4}	-7.2	-1.3

Fraction Burnup Deficit of and Characteristic Relaxation Times
 $(nt)_I$, $(vt)_I$ for Various Temperatures

It is convenient to scale the fraction burnup f with f_M . In this way we construct Fig. 4 which allows plotting all the results together. The left-hand portion of the plot corresponds to short times and gives constant ratios

$$f/f_M = \langle \sigma v \rangle_0 / \langle \sigma v \rangle_M$$

corresponding to negligible relaxation from the initial delta-function distribution. The right-hand portion of the chart corresponds to long times and shows saturation of f/f_M to unity. The low-temperature cases rise to saturation closer to the left because of the $\langle \sigma v \rangle_M$ in the time-like scaling.

APPLICATION

The data of Fig. 4 are intended to allow the postcorrection of computed results which assume Maxwellian distributions. As an interesting application, we apply these tail-filling corrections to the results of the initial condition burn-study² which we have also modified to estimate the effects of fast ion losses.⁴ The two corrections overlaid on the (Maxwellian) computer simulations are shown in Fig. 5. We see that there is a linear region separating the bootstrap heating and central ignition regime at high $\rho R > 1 \text{ gm cm}^{-2}$ from the region of important corrections at low $\rho R < 0.01 \text{ gm cm}^{-2}$.

This separation justifies the neglect of nonlinear processes in the present analysis. The values of $f \ll 1$ justify the neglect of fuel depletion. From inspection of the two results, it is clear that in most cases the fast ion loss is the more important effect. In those cases in which the finite tail-filling is more important it is only a 20 to 30% effect.

COMBINED MODEL

The self-consistent problem including both the loss of fast ions from the tail and evolution of the distribution function from an initial state is accomplished by adding an appropriate loss term to the Fokker-Planck treatment. What is not so clear, however, is how one should treat the bounding conditions: are particles lost, is energy lost, etc.? A complete treatment would actually allow fluxes of both particles and energy, with the boundary conditions being specified as functions of time from a coupled hydrodynamics calculation. Such a major undertaking does not appear justified since we have found the non-Maxwellian effects to disappear at significant compressions ($\rho R \gg 0.01 \text{ gm cm}^{-2}$).

In the spirit of postcorrections to hydrodynamics calculations which assume Maxwellian distributions, we have performed some combined-ion loss

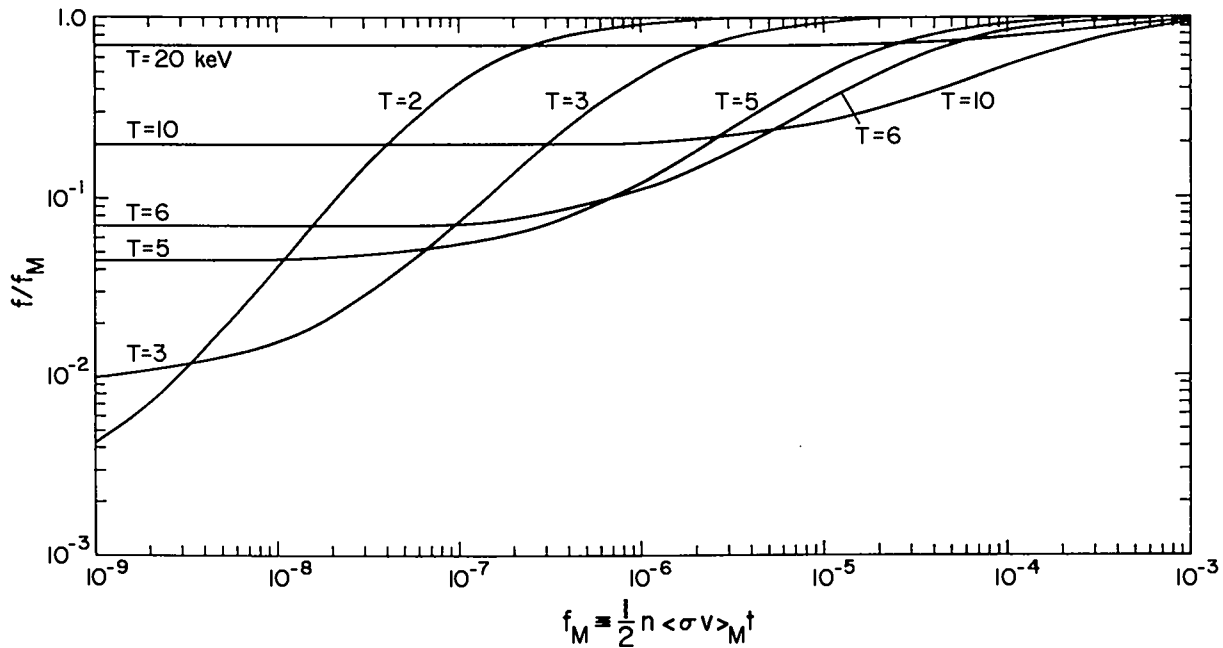


Fig. 4 Fractional burnup ratio f/f_M vs the a priori functions burnup f_M .

and ion evolution-calculations. For the loss term we consider the loss of particles by diffusion from a uniform sphere. Using well-known results from reactor theory⁹, the loss is

$$\frac{1}{N} \frac{dN}{dt} = \frac{\lambda v}{3N} \nabla^2 N$$

Taking $\frac{1}{N} \nabla^2 N$ to be constant over the sphere of radius R , we have

$$\frac{1}{N} \nabla^2 N = \frac{\pi^2}{R^2}, \text{ so that } \frac{1}{2} \frac{dN}{dt} = \frac{\pi^2}{3} \frac{\lambda v}{R^2}$$

for each group of ions at speed v . We have included this term in the computer code, with $\lambda(v)$ evaluated as in Ref. 4. Otherwise, the Fokker-Planck calculations proceeded as described above.

For the case of an initial speed at the equivalent of $T = 3$ -keV energy, the evaluation of the $\langle \sigma v \rangle$ value is shown in Fig. 6. An overlay of this data with the 3-keV data from Fig. 1 shows no noticeable difference between the $\rho R = 10^{-2} \text{ gm cm}^{-2}$ and the no-loss results. That is, $\rho R = 10^{-2} \text{ gm cm}^{-2}$ is effectively thick as we have already concluded. As the tail fills out, from the initial delta-function toward regions of v with significant par-

ticle loss, we notice the values of $\langle \sigma v \rangle$ begin to drop. The $\rho R = 10^{-4} \text{ gm cm}^{-2}$ case shows an actual decline in $\langle \sigma v \rangle$ with time from a maximum at about 10 collision times. This is accompanied by significant cooling, as may be seen from the values of $T = M \langle v^2 \rangle / 3k$ which are also plotted. Had the problem been done with the distributions renormalized to maintain a constant T , the results would clearly be different. In a physical problem there would, of course, be an important heat loss and a decrease in fuel pressure; these would be important to the hydrodynamics.

The fractional burnup values for the 3-keV case are shown in Fig. 7. For the very thin $\rho R = 10^{-4} \text{ gm cm}^{-3}$ case, the fractional burnup becomes nearly constant as the $\langle \sigma v \rangle$ value drops. The data in Fig. 7 may be used to postcorrect hydrodynamics-burn calculations in the same way as that in Figs. 3 or 4. Simple bare pellets are known to effectively disassemble in an expansion time²

$$\tau_e = R/4C_s, \quad C_s = \text{sound speed.}$$

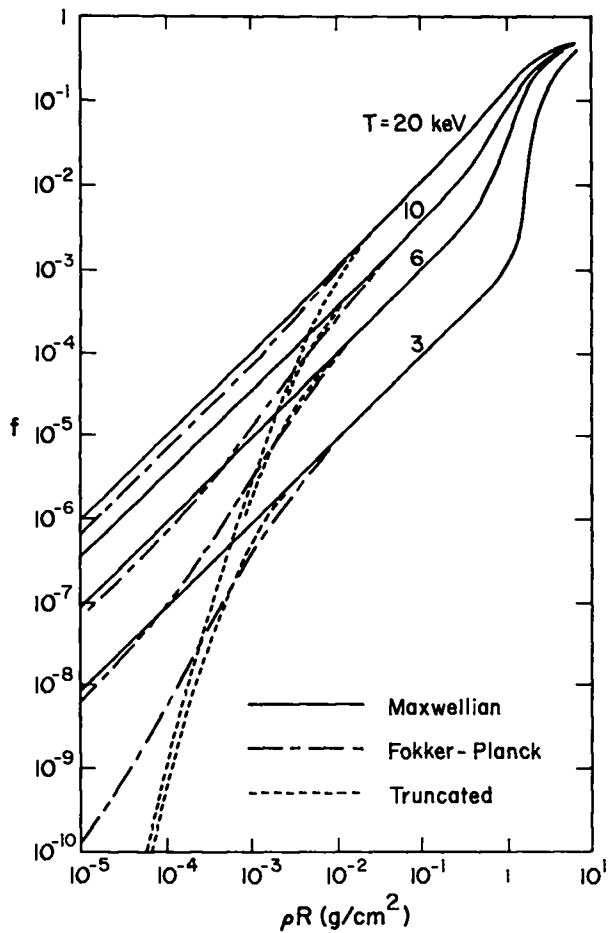


Fig. 5 Application of data of Fig. 4 to curves of fraction burnup from a burn study (Ref. 2). Also shown are corrections due to fast-ion losses from Ref. 4.

For 1.0- μ g DT spheres at 3-keV, this works out to approximately

$$\tau_e = 1.4 \times 10^{14} (\rho R) \text{ (cgs units) .}$$

In all cases the disassembly is so rapid as to occur before the fractional burnup deviates significantly from the thick ($\rho R \geq 10^{-2} \text{ gm cm}^{-2}$) result. That is, in these problems the truncation of the distribution loss by ion loss will have no effect. In structured systems, however, the confinement times may be considerably longer and the deviations from the thick-case results may be important.

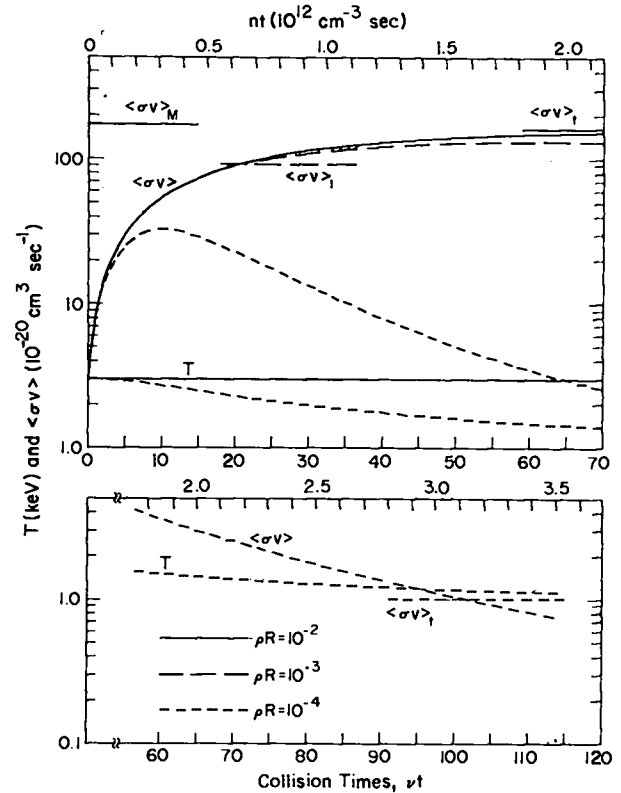


Fig. 6 Time evolution of fusion reactivity $\langle \sigma v \rangle$ and the mean energy T for T = 3-keV initial distribution; $\langle \sigma v \rangle_M$ corresponds to a Maxwellian distribution; $\langle \sigma v \rangle_t$ corresponds to truncated distributions as in Ref. 4.

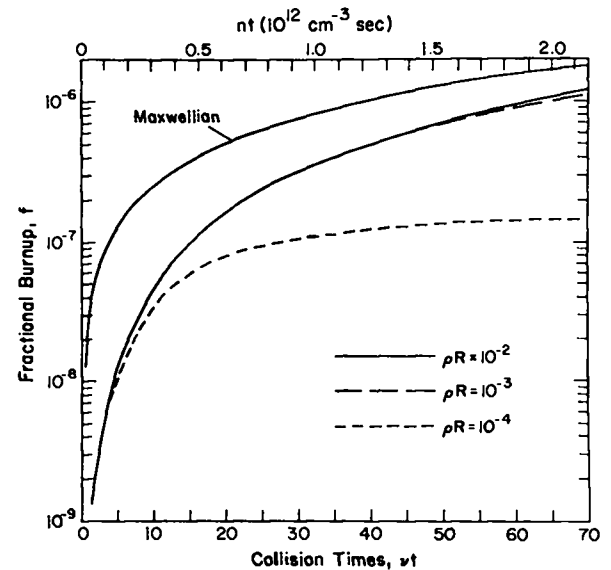


Fig. 7 Fractional burnup integrated from data of Fig. 6.

Similar results for the case of an initial speed at the equivalent speed of $T=6$ -keV energy are shown in Figs. 8 and 9. In this case the $\langle\sigma v\rangle$ values for $\rho R = 10^{-4}$ gm cm $^{-2}$ are seen to drop very quickly, making the fractional burnup almost independent of time after the initial overshoot.

Also indicated in Figs. 6 and 8 are the values of $\langle\sigma v\rangle_t$ for truncated ion distributions which were found in Ref. 4. We see that while the results of Ref. 4 were correct in indicating the ranges of ρR for serious ion loss effects and for no such effects, the numerical values $\langle\sigma v\rangle_t$ obtained are only rough guides. Eventually the $\langle\sigma v\rangle$'s obtained here will saturate to values below the $\langle\sigma v\rangle_t$'s, but only after very long times. The time dependence of $\langle\sigma v\rangle$ prior to the saturation is very strong, especially for the $\rho R = 10^{-4}$ gm cm $^{-2}$ cases, indicating a need for time-dependent evolutionary calculations.

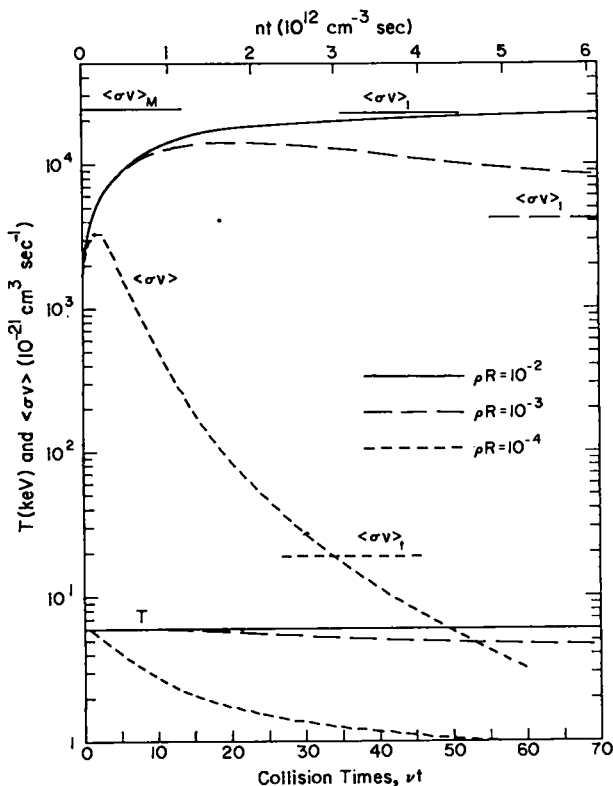


Fig. 8 Time evolution of the fusion reactivity $\langle\sigma v\rangle$ and the mean energy T for $T = 6$ keV initially with fast ion losses; $\langle\sigma v\rangle_M$ and $\langle\sigma v\rangle_t$ are as in Fig. 6.

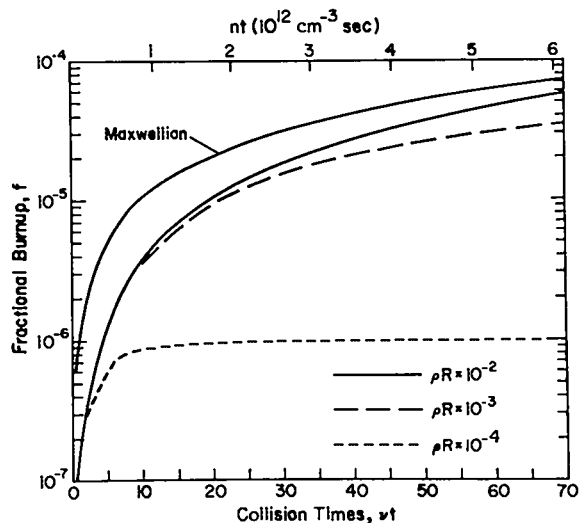


Fig. 9 Fraction burnup integrated from data of Fig. 8.

Having explored the ion loss effect⁴, the time evolution of the distributions, and the combined problem, we feel that we understand the observed yields, which are below a priori (Maxwellian) estimates.¹⁰ It is possible to construct hydrodynamics-burn computer codes which take proper account of these effects, using the methods outlined here. However, in view of these effects becoming unimportant above $\rho R = 0.01$ gm cm $^{-2}$, the effect does not appear justified. It is important, however, to have resolved the question of why the current experimental yields lie below the Maxwellian results.

REFERENCES

1. J. S. Clarke, H. N. Fisher, and R. J. Mason, "Laser-Driven Implosion of Spherical DT Targets to Thermonuclear Burn Conditions," *Phys. Rev. Lett.* **30**, 89, (1973).
2. G. S. Fraley, E. J. Linnebur, R. J. Mason, and R. L. Morse, "Thermonuclear Burn Characteristics of Compressed Deuterium-Tritium Microspheres," *Phys. Fluids* **17**, 474 (1974).
3. J. Nuckolls, L. Wood, A. Thiessen, and G. Zimmerman, "Laser Compression of Matter to Super-High Densities: Thermonuclear (CTR) Applications," *Nature (London)* **239**, 139 (1972).
4. D. B. Henderson, "Burn Characteristics of Marginal Deuterium-Tritium Microspheres," Los Alamos Scientific Laboratory report LA-5603-MS, *Phys. Rev. Lett.* **33**, 1142 (1974).
5. M. N. Rosenbluth, W. M. MacDonald, and D. L. Judd, "Fokker-Planck Equation for Inverse-Square Force," *Phys. Rev.* **107**, 1 (1957).

6. This is very similar to the method used by W. M. MacDonald, M. N. Rosenbluth, and W. Chuck, "Relaxation of System of Particles with Coulomb Interactions," Phys. Rev. 107, 350 (1957).
7. L. Spitzer, "Physics of Fully Ionized Gases," (Interscience, New York, 1956) p. 78.
8. B. H. Duane, Battelle Northwest Laboratory, unpublished data, 1972.
9. A. G. Petschek, USERDA, personal communication (1975).
10. H. Brysk and P. Hammerling, "DT Fusion with Microshells," Phys. Rev. Lett. 34, 502 (1975).